D会場: 11/25 AM1 (9:15-10:45)

9:15~9:30:00

3次元節点変位を用いたアダプティブ六面体有限要素法による CSEM モデリングと 熱水系の変動解析への応用

#北岡 紀広 ¹⁾, 小川 康雄 ^{1,2)}, Caldwell T. Grant³⁾, 石須 慶一 ⁴⁾, 南 拓人 ⁵⁾, Kirkby Alison³⁾ 「東京科学大学, ⁽² 東北大学, ⁽³Earth Sciences New Zealand, ⁽⁴ 九州大学, ⁽⁵ 神戸大学

An Adaptive Hexahedral FEM with 3D Nodal Displacement for CSEM Modeling and Its Application to a Hydrothermal System

#Norihiro Kitaoka¹⁾, Yasuo Ogawa^{1,2)}, T. Grant Caldwell³⁾, Keiichi Ishizu⁴⁾, Takuto Minami⁵⁾, Alison Kirkby³⁾
⁽¹Institute of Science Tokyo, ⁽²Tohoku University, ⁽³Earth Sciences New Zealand, ⁽⁴Kyushu University, ⁽⁵Kobe University)

The Finite Element Method (FEM) is a powerful tool for 3D electromagnetic modeling in geophysical exploration methods such as CSEM and MT. To balance computational cost and accuracy, adaptive FEM techniques using octree-based mesh refinement have been developed. While both tetrahedral and hexahedral elements are used, hexahedral elements are often preferred for their ability to align with geological layers and maintain numerical stability. However, previous hexahedral adaptive FEM approaches have primarily been limited to vertical nodal displacement for representing complex topography and have used linear approximations for the transfer function at the boundaries, which can pose challenges in accurately modeling finite-length sources and suppressing artificial reflections.

In this study, we significantly extend this methodology to overcome these limitations. First, we have developed a new hexahedral adaptive mesh generation technique that incorporates full 3D nodal displacement. This allows for the high-fidelity representation of complex features such as finite-length CSEM sources and lake bathymetry without sacrificing mesh quality. The 3D mesh deformation is achieved through a two-step process: we first calculate 2D displacements on the surface mesh to match target features using a non-linear FEM, and then compute the full 3D displacements after incorporating elevation data. Second, we have implemented an improved boundary condition using a transfer function composed of a superposition of exponential functions ($\exp(\pm ikx)$). This condition simulates an outgoing wave, effectively minimizing artificial reflections from the model boundaries. Compared to the conventional Dirichlet boundary condition, our approach achieves high accuracy over a wider area of the computational domain, even with a smaller model space.

In this presentation, we will first validate our new code by comparing its numerical results with the analytical solution for a finite-length dipole CSEM source. We will then present a key application of the code to the continuous CSEM data acquired at Inferno Crater Lake, New Zealand, in 2023. This site is known for its vigorous 40-day cycle of water level and temperature fluctuations, suggesting dynamic subsurface processes. We use our forward modeling to quantitatively interpret the observed resistivity variations that are synchronized with the lake's cycle, and discuss the implications for the dynamics of the shallow high-resistivity layer, interpreted as a vapor-dominated zone.

CSEM 法や MT 法など 3 次元電磁探査の電磁場計算において、有限要素法(FEM)は複雑な地下構造をモデル化するための強力なツールである。特に、計算コストと精度の両立を目指し、八分木構造でメッシュを局所的に細分化するアダプティブ FEM が開発されてきた。そのメッシュ要素には四面体と六面体があるが、六面体要素は層状構造の表現に優れ、数値的な安定性も高いことから、地質学的モデルとの親和性が高い。しかし、従来の六面体アダプティブ FEM では、地形などの複雑な形状を表現するために鉛直方向のみの節点変位に限定された手法や、伝達関数を線形近似する手法が主流であり、有限長の電流源や急峻な地形の表現、計算領域の境界での人工的な反射波の抑制に課題があった。

本研究では、これらの課題を克服するため、手法を大幅に拡張した。第一に、水平方向を含む任意の3次元節点変位を許容する六面体アダプティブメッシュ生成手法を開発した。これにより、送信ダイポールや湖底地形といった複雑な形状を、メッシュの品質を損なうことなく忠実にモデルへ組み込むことが可能となった。このメッシュ変形は、まず八分木分割された空間の地表面メッシュに対し、非線形有限要素法を用いて目標形状に合わせた2次元的な変位を計算し、その後、標高情報を加えて3次元空間全体の変位を計算するという、2段階のプロセスで実現した。第二に、計算領域の境界条件として、波動が計算領域の外側へ透過していく物理的状況を模擬するため、指数関数型(exp(± ikx))の伝達関数を導入した。これは人工的な反射波の発生を効果的に抑制し、従来のディリクレ境界条件に比べて、より狭い計算領域でも解析解と広範囲で一致する高精度な計算を可能にする。

本発表では、まず開発したコードの精度を検証するため、有限長ダイポールソースによる CSEM 法の解析解と計算結果を比較し、その有効性を示す。さらに、このコードを 2023 年にニュージーランド・インフェルノ火口湖で取得された CSEM 連続観測データに適用した結果を報告する。この湖では約 40 日周期の活発な水位・水温変動が観測されており、地下の蒸気卓越層のダイナミクスが示唆されている。我々の観測で捉えられた湖水位変動と同期した比抵抗変動を、開発したフォワードモデリングを用いて定量的に説明し、その変動を引き起こす蒸気卓越層の厚さや形状の変化について議論する。

D会場: 11/25 AM1 (9:15-10:45)

9:30~9:45:00

塩水飽和岩石における三軸変形中の電気抵抗率異方性

#鈴木 健士 $^{1)}$, 宗 慈瑛 $^{2)}$, 赤松 祐哉 $^{3)}$, 澤山 和貴 $^{2)}$, 片山 郁夫 $^{4)}$ $^{(1)}$ 産業技術総合研究所, $^{(2)}$ 京都大学地球熱学研究施設, $^{(3)}$ 海洋研究開発機構, $^{(4)}$ 広島大学

Electrical Resistivity Anisotropy in Brine-Saturated Rocks during Triaxial Deformation

#Suzuki Takeshi¹⁾, Jiei So²⁾, Yuya Akamatsu³⁾, Kazuki Sawayama²⁾, Ikuo Katayama⁴⁾

⁽¹⁾National Institute of Advanced Industrial Science and Technology, ⁽²⁾Institute for Geothermal Sciences, Kyoto University, ⁽³⁾Japan Agency for Marine-Earth Science and Technology, ⁽⁴⁾Hiroshima University

Electrical resistivity anisotropy within the crust serves as a crucial geophysical indicator reflecting the distribution of stress-aligned cracks and fault zones. Recent advances in electromagnetic methods have enabled the identification of numerous anisotropic electrical resistivity structures in both continental and oceanic crusts, revealing the presence of cracks aligned with regional stress fields. These cracks typically develop with their long axes parallel to the direction of maximum principal stress, creating anisotropy that reflects the dominant stress regime of the region. To interpret resistivity anisotropy observed in the field, it is essential to validate through resistivity anisotropy measurements under controlled differential stress conditions. However, previous studies have primarily measured resistivity along the maximum stress axis direction, and comprehensive experimental methods for evaluating resistivity anisotropy have not been established. Therefore, this study developed a novel methodology for measuring anisotropic electrical resistivity during triaxial deformation experiments and elucidated the evolution of resistivity anisotropy throughout the deformation process.

For radial resistivity measurements in cylindrical rock samples, the effective cross-sectional area of electrical current was determined through three-dimensional electrostatic field numerical simulations. Evaluation of electrode materials under high-pressure conditions confirmed that Ag/AgCl electrodes demonstrated superior performance. The developed experimental method enabled simultaneous measurement of both axial and radial resistivities during triaxial deformation.

The method was applied to triaxial compression tests on Aji granite (confining pressure 20 MPa, pore pressure 10 MPa). As a result, the development of resistivity anisotropy throughout the entire deformation process could be monitored. During the early deformation stage, the increase in radial resistivity was more pronounced than in the axial direction. This can be interpreted as closure of pre-existing cracks oriented at high angles to the compression axis. In the middle stage of deformation, the decrease in axial resistivity became more pronounced than in the radial direction. This is interpreted as the development of new cracks parallel to the stress axis. At least the resistivity anisotropy observed in the early stages of deformation is considered uniform throughout the sample, and the results obtained from this study can provide data for interpreting resistivity anisotropic structures observed in field surveys.

地殻内の電気比抵抗異方性は、応力場に配向したクラックや断層帯の分布を反映する重要な地球物理学的指標である。近年の電磁気学的手法の進展により、大陸地殻や海洋地殻において、地域応力場に沿って配列したクラックの存在を示す電気比抵抗異方性が数多く報告されている。これらのクラックは一般に最大主応力方向に長軸をもつように発達し、その領域に卓越する応力状態を反映した異方性を生じる。このような野外で観測される比抵抗異方性を解釈するには、制御された差応力条件下における比抵抗異方性の実験的検証が不可欠である。しかし従来の研究は主として最大応力軸方向の比抵抗測定に限られており、比抵抗異方性を評価する実験手法は確立されていなかった。

本研究では、変形試験中の岩石における電気比抵抗異方性の計測手法を新たに開発し、変形過程における比抵抗異方性の進展を明らかにした。具体的には、円筒形岩石試料における周方向の比抵抗測定のため、3次元静電場の数値シミュレーションにより、周方向の電流の有効断面積を算定した。また、高圧環境下での電極材料評価を行い、Ag/AgCI電極が優れた性能を有することを確認した。これらの成果に基づき、軸方向と周方向の比抵抗を三軸変形試験中に同時測定することが可能となった。

開発した手法は、庵治花崗岩を用いた三軸変形試験(封圧 20 MPa、間隙水圧 10 MPa)に適用された。その結果、変形過程に伴う比抵抗異方性の発達をモニタリングすることに成功した。変形初期には、軸方向に比べ周方向の比抵抗増加が顕著であり、これは圧縮軸に対して高角度に配向する既存クラックの閉鎖によると解釈される。一方、変形中盤では、周方向よりも軸方向の比抵抗低下が顕著であり、応力軸に平行な新規クラックの発達を反映すると考えられる。変形初期に観察される比抵抗異方性は試料全体に一様にあらわれると考えられ、本研究で得られた成果は、野外探査における比抵抗異方性構造の解釈に重要な基礎データとなりうる。

D会場: 11/25 AM1 (9:15-10:45)

9:45~10:00:00

#宋 晗 $^{1,2)}$, 于 鵬 $^{1)}$, 臼井 嘉哉 $^{2)}$, 上嶋 誠 $^{2)}$, Diba Dieno $^{2,3)}$, 張 羅磊 $^{1)}$, 趙 崇進 $^{1)}$ 「同済大学、海洋地質国家重点研、 $^{(2)}$ 東京大学、地震研究所、 $^{(3)}$ 都柏林高等研究院

Three-dimensional Magnetotelluric Inversion based on a Data Space variant of Akaike's Bayesian Information Criterion

#Han Song^{1,2)}, Peng Yu¹⁾, Yoshiya USUI²⁾, Makoto UYESHIMA²⁾, Dieno Diba^{2,3)}, Luolei Zhang¹⁾, Chongjin Zhao¹⁾
⁽¹State Key Laboratory of Marine Geology, Tongji University, ⁽²Earthquake Research Institute, The University of Tokyo, ⁽³The Dublin Institute for Advanced Studies

We develop a three-dimensional (3-D) magnetotelluric (MT) inversion method based on Akaike's Bayesian Information Criterion (ABIC), which statistically determines the optimal regularization parameter that balances the prior constraints and data fitting, and therefore controls the smoothness of the final model by incorporating the entropy-maximization theorem into Bayesian statistics. To mitigate the high computational cost of calculating the ABIC indicator, we introduce a low-rank transformation, similar to that used in model-to-data space inversions, resulting in a data-space variant of ABIC. This adaptation significantly reduces computational complexity, facilitating the practical application of ABIC in 3-D MT inversions. Our discussion on the methodology and its application begins with a theoretical analysis of the proposed inversion method, including the underlying assumptions, the mathematical foundations of this statistical framework, a detailed derivation of the data-space ABIC formulation, and the procedure for obtaining maximum likelihood solutions in 3-D MT inversion. We then assess the method's performance using synthetic data, evaluate its stability under different inversion configurations, and benchmark it against other inversion strategies, including those based on the L-curve criterion, the cooling approach, and the original ABIC in model space. We demonstrate that the proposed inversion based on the data-space ABIC formulation yields stable performance across various configurations and offers improved objectivity compared to L-curve and cooling-based inversions. It also gains a substantial computational advantage over the original model-space ABIC formulation, achieving over a 70-fold speedup in synthetic tests while preserving statistical rigor. This facilitates a smooth transition of ABIC-based MT inversion from 2-D to 3-D and also opens the door to its broader application in other large-scale inverse problems. Finally, we briefly consider a field data application of the proposed 3-D method to the Yellowstone - Snake River Plain region using EarthScope USArray MT data to showcase its practical applicability.

D会場: 11/25 AM1 (9:15-10:45)

10:00~10:15:00

#LIMBONG Gita Amelia Marianto^{1,2)}, NURHASAN Nurhasan²⁾ (1 東大地震研、⁽² バンドン工科大

Two-Dimensional MT Inversion with Impedance and Tipper Response using KLU, Cholesky, and BiCGSTAB Solvers

#Gita Amelia Marianto LIMBONG^{1,2)}, Nurhasan NURHASAN²⁾
⁽¹Earthquake Research Institute, The University of Tokyo, ⁽²Bandung Institute of Technology

This study develops a two-dimensional magnetotelluric inversion program utilizing both impedance and tipper responses. The forward modeling in the inversion framework is carried out using a finite element numerical method based on nodes and unstructured triangular elements to solve the electromagnetic field problem formulated as a second-order differential equation. The inversion process is implemented using the Gauss-Newton algorithm, along with several matrix solver algorithms (KLU, Cholesky, and BiCGSTAB) to evaluate computational accuracy and efficiency. Validation of the forward modeling program was conducted using standard COMMEMI 2D-0 and COMMEMI2D-1 models. The average percentage error of apparent resistivity for the COMMEMI2D-0 model ranged from 5.06% to 6.44%, while for the COMMEMI2D-1 model, the range was between 1.80% and 1.95%. Further validation of the inversion program was performed using synthetic Earth models, including a homogeneous Earth model, a layered Earth model, and an Earth model with anomalies. The results from the three matrix solver algorithms show that while different solvers yield similar inversion accuracy, they differ in computational efficiency, particularly in terms of iteration time and memory usage. Among them, the KLU algorithm demonstrated the best performance, with shorter iteration times (200 – 3200 seconds) and lower memory usage (2.0 – 3.1 GB) compared to the others. In addition, the integration of tipper responses significantly improved the modeling results for Earth structures with lateral resistivity variations, producing more accurate outcomes than those obtained without tipper integration.

D会場: 11/25 AM1 (9:15-10:45)

10:15~10:30:00

比抵抗モデルにおける対応するt検定を用いた比抵抗信頼区間推定について

#市來 雅啓 ¹⁾, Siripunvaraporn Weerachai²⁾

(1 東北大, ⁽² マヒドン大学

On statistical confidence interval inference of resistivity for a target block in optimal resistivity model using a paired t-test

#Masahiro Ichiki¹⁾, Weerachai Siripunvaraporn²⁾
⁽¹Tohoku University, Japan, ⁽²Mahidol University, Thailand

This presentation proposes a scheme for the statistical confidence interval inference of the subsurface electrical resistivity model using a paired t-test assisted by forward modeling. The method assesses the confidence interval of resistivity for a target block in optimal model obtained by inversion. The target block consists of several model elements, and arbitrarily defined by an operator. By changing resistivity of the target block, and executing the forward modeling, we evaluate the confidence interval of resistivity for the target block using a paired t-test to assess the change in data misfit. Previous studies used the F-test to estimate the confidence interval of resistivity by assessing the change in chi-square misfit. However, the F-test requires the chi-square misfits must follow chi-square distributions, and the chi-square misfit actually does not follow any chi-square distribution in many cases. The proposed method using the t-test is to evaluate the change in mean of z misfit, which is defined by in-phase and quadrature-phase of magnetotelluric impedance and geomagnetic transfer function misfit normalized by standard data error.

This presentation shows an example to apply this method to estimate the confidence interval of resistivity of the magma/hydrothermal reservoir beneath Mt. Azuma (Ichiki et al., 2021), and reveals that the confidence interval obtained using the F-test is likely to overestimate the confidence interval.

Acknowledgment: This study was inspired by discussions with Dr. Noriko Tada, and we are grateful to Professors Ogawa and Uyeshima for their valuable comments.

MT インピーダンスと地磁気変換関数の逆問題で得られた地下比抵抗最適モデル中の特定の領域に対して、対応する t 検定を用いた比抵抗値の対信頼区間推定を提案する。最適比抵抗モデル中の特定の領域は、特徴的な構造や地質学的に重要な領域を解析者が任意に定め、その領域の比抵抗値を変化させて順問題を実施しながらデータの合いを統計的検定によって評価する。これまでの研究では、この枠組みを用いた比抵抗値の信頼区間推定では X 二乗ミスフィットの変化を F 検定によって評価しながら信頼区間を推定していた。しかしながら F 検定は、X 二乗ミスフィットが X 二乗分布に従う場合にのみ適用できるが、多くの逆問題の最適解による X 二乗ミスフィットは X 二乗分布に従わない。新しい枠組みでは、データの合いをここでは X ミスフィットと定義したミスフィットの平均が変化するかを対応する t 検定で評価することで比抵抗の信頼区間推定を行う。ここでの X ミスフィットとは、MT インピーダンスと地磁気変換関数の実部と虚部のミスフィットをデータ標準誤差で割ったものである。

本発表ではこの手法を吾妻山下のマグマ・熱水だまりと解釈される低比抵抗体に対して適用し比抵抗の信頼区間を求めた例を発表する。また従来のF検定で求めた信頼区間とも比較し、F検定で求めた信頼区間が過大に見積もられている可能性があることを示す。

謝辞: 本研究は多田訓子博士との議論により着想を得た。小川康雄、上嶋誠、両教授からは有益なコメントを得た。記して感謝します。

D会場: 11/25 AM1 (9:15-10:45)

10:30~10:45:00

2011年東北地震津波の際の電場変動を用いた神津島の比抵抗構造推定

#武林 哲志 1), 南 拓人 1), 上嶋 誠 2)

(1 神戸大学大学院理学研究科, (2 東京大学地震研究所

Estimation of Kozushima subsurface resistivity structure using tsunami-induced electric fields from the 2011 Tohoku earthquake

#Tetsuji TAKEBAYASHI¹⁾, Takuto MINAMI¹⁾, Makoto UYESHIMA²⁾

⁽¹Graduate School of Science, Kobe University, ⁽²Earthquake Research Institute, The University of Tokyo

When conductive seawater moves through the geomagnetic field during a tsunami, tsunami-generated electromagnetic (TGEM) variations occur (e.g., Tyler, 2005). The TGEM variations can be observed both on land and at the seafloor (e.g., Minami et al., 2017). During the 2011 Tohoku earthquake tsunami, significant electric field variations were detected on Kozushima, a volcanic island in the Izu Islands, with the maximum occurring almost simultaneously with the tide gauge peak (Nakatani, 2015, Graduation thesis in Tokyo Gakugei University). While tsunami-generated electric (TGE) fields observed at the seafloor are little affected by the subseafloor resistivity (Shimizu and Utada, 2015), they are strongly influenced by the subsurface resistivity on islands (Minami, 2024; Shibahara, 2022, Graduation thesis in Kobe University). In this study, we estimate the subsurface resistivity structure of Kozushima using TGE variation data during the 2011 Tohoku earthquake tsunami.

On Kozushima, electric potential observations utilizing two long dipoles were conducted by Dr. Yoshiaki Orihara and Mr. Yoichi Noda as part of the "Earthquake International Frontier Research" program of the Science and Technology Agency. The two dipoles were oriented southeast-northwest (2.382km) and northeast-southwest (2.137km), providing two components of potential difference. The observed potential differences were divided by the dipole lengths to obtain two components of the electric field in the northwestward and southwestward directions. To remove variations unrelated to tsunamis from the observed data, we applied the RRRMT method using magnetic data at Changchun, China, reducing magnetic storms effect, following the method in Minami et al. (2017).

The TGE variations on Kozushima were simulated using the time-domain finite-element electromagnetic fields simulation code TMTGEM (Minami et al., 2017). The tsunami velocity field used as input was calculated with JAGURS (Baba et al., 2017), a tsunami simulation code based on linear dispersive wave theory. For the TGE simulations, a tetrahedral mesh was constructed with a minimum edge length of about 200 m around Kozushima.

As a first test, we used homogeneous resistivity structures and performed simulations with resistivity values of 10, 100, and 1000 Ω m. None of these cases reproduced the observed data. The northwest electric field variation showed a negative excursion consistent with the observation, whereas the southwestward component exhibited a positive peak for all resistivity values, in contrast to the observed data, which did not display a distinct peak. Next, we constructed a resistivity model based on geological evidence that eruption centers aligned in a southeast-northwest direction (Taniguchi, 1977), and on previous electromagnetic surveys suggesting the presence of groundwater (Orihara et al., 2010). We assumed a southeast-northwest trending low-resistivity anomaly embedded within a high-resistivity background. Specifically, the background resistivity was set to $1000~\Omega$ m and a $10~\Omega$ m anomaly extending from the surface down to 300 m below sea level was introduced. This model successfully reproduced the northwestward electric field variation, as in the homogeneous cases, while also improving the agreement with the observed southwestward variation. These results suggest the presence of a low-resistivity region within the central part of Kozushima, embedded in the homogeneous high-resistivity background structure.

This study demonstrates the potential of using TGE variations as a new approach for subsurface structure estimation, revealing a low-resistivity anomaly beneath Kozushima. While the structures around the dipoles have been constrained, regions farther away remain poorly resolved. Future work will focus on improving estimation accuracy by focusing on regions with higher sensitivity and by refining the tsunami simulations that provide input to the electric field calculations.

11:05~11:35:00

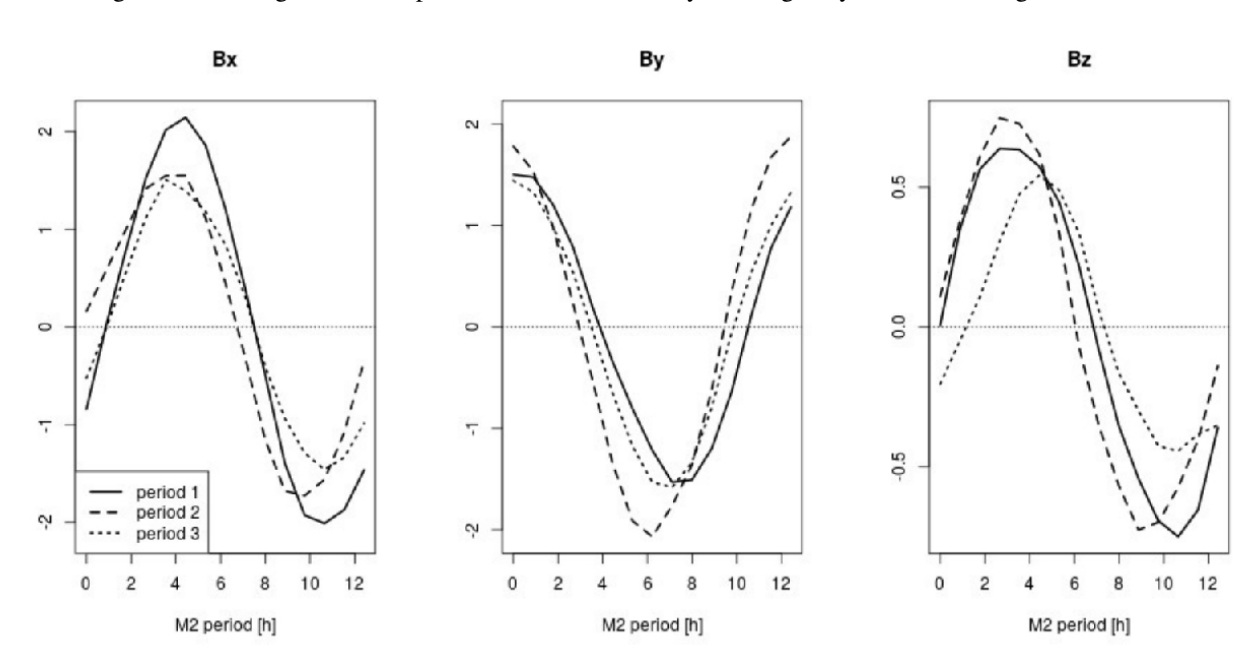
#Saynisch Jan¹⁾, Baerenzung Julien²⁾, Hornschild Aaron¹⁾, Irrgang Christopher³⁾
(¹GFZ-Potsdam, ⁽²TU-Berlin, ⁽³RKI

Electromagnetic ocean tidal signals for oceanic monitoring

#Jan Saynisch¹⁾, Julien Baerenzung²⁾, Aaron Hornschild¹⁾, Christopher Irrgang³⁾
⁽¹GFZ Helmholtz Centre for Geosciences, ⁽²Technical University Berlin, ⁽³Robert Koch Institute

As currently the oceans absorb 90% of Earth's excess heat, the importance of estimating the oceanic heat budget cannot be overestimated. Knowing changes in this process as early as possible is highly important. Changes in the heat uptake rate or even raised re-emissions will have a large impact on the future climate. Already now we see a rising number of oceanic heat waves at the ocean surface which lead to corral bleaching and other severe impacts on the ecosystem. Likewise, knowing the freshwater input into the oceans, e.e., from the melting glaciers is highly important as it might lead to tipping of the overturning circulation.

Oceanic electromagnetic (EM) tidal signals are in principle sensitive to both temperature and salinity of oceanic waters. If changes of these tidal signals could be accurately detected and related to climate change induced variations of the sea water properties then the analysis of these measurements could provide a highly significant contribution to oceanic monitoring, prediction and mitigation. We will report on the progress made in EM tidal signal detection and separation from satellites and in-situ observations. Furthermore, we will advertise the exploration of EM tidal signals for oceanic monitoring by demonstrating and discussing the next steps in EM ocean tidal analysis that go beyond the mere signal detection.



D会場: 11/25 AM2 (11:05-12:35)

11:35~11:50:00

能登半島北部の3次元比抵抗構造と地震活動の関係

#吉村 令慧 $^{1)}$, 平松 良浩 $^{2)}$, 後藤 忠徳 $^{3)}$, 笠谷 貴史 $^{4)}$, 宮町 凜太郎 $^{1)}$, 中川 潤 $^{1)}$, 山下 凪 $^{3)}$, 天野 玲 $^{3)}$, 深田 雅人 $^{2)}$, 杉井 天音 $^{2)}$, 福岡 光輝 $^{2)}$, 乾 太生 $^{1)}$, 山崎 健一 $^{1)}$, 小松 信太郎 $^{1)}$, 岩堀 卓弥 $^{1)}$, 吉川 昌宏 $^{1)}$, 大田 優介 $^{4)}$, 小倉 訓 $^{4)}$, 木谷 洋一郎 $^{2)}$, 小木曽 正造 $^{2)}$, 鷹巣 真琳 $^{2)}$, 岡村 隆行 $^{2)}$, 櫻井 未久 $^{3)}$, 北谷 凌一 $^{3)}$, 波岸 彩子 $^{1)}$, 長岡 愛理 $^{1)}$, 達山 康人 $^{1)}$, 澤田 明 宏 $^{2)}$, 張 策 $^{2)}$, 陣出 湧也 $^{2)}$, 大島 由有希 $^{3)}$

(1 京大防災研, (2 金沢大学, (3 兵庫県立大学, (4 海洋研究開発機構

Three-Dimensional Resistivity Structure and Its Relation to Seismic Activity in the Northern Noto Peninsula

#Ryokei Yoshimura¹⁾, Yoshihiro Hiramatsu²⁾, Tada-nori Goto³⁾, Takafumi KASAYA⁴⁾, Rintarou Miyamachi¹⁾, Jun Nakagawa¹⁾, Nagi Yamashita³⁾, Rei Amano³⁾, Masato Fukata²⁾, Amane Sugii²⁾, Mitsuteru Fukuoka²⁾, Taisei Inui¹⁾, Kenichi YAMAZAKI¹⁾, Shintaro Komatsu¹⁾, Takuya Iwahori¹⁾, Masahiro Yoshikawa¹⁾, Yusuke OHTA⁴⁾, Satoshi Ogura⁴⁾, Yoichiro Kitani²⁾, Shozo Ogiso²⁾, Marin Takasu²⁾, Takayuki Okamura²⁾, Miku Sakurai³⁾, Ryoichi Kitatani³⁾, Ayako Namigishi¹⁾, Airi Nagaoka¹⁾, Yasuto Tatsuyama¹⁾, Akihiro Sawada²⁾, Ce Zhang²⁾, Yuya Jinde²⁾, Yuki Oshima³⁾

(¹Disaster Prevention Research Institute, Kyoto University, (²Kanazawa University, (³University of Hyogo, (⁴Japan Agency for Marine-Earth Science and Technology

On January 1, 2024, a large intraplate earthquake (Mw7.5) struck the northern part of the Noto Peninsula in north-central Japan, causing widespread damage due to strong ground motions and a tsunami. Prior to this catastrophic earthquake, an intense earthquake swarm and localized non-steady crustal deformation had been observed continuously since late 2020 in the region, which is a non-volcanic area. The swarm activity persisted, producing several M5-class earthquakes, including an M6.5 on May 5, 2023, before culminating in the Mw 7.5 earthquake. In 2007, an Mw 6.7 earthquake also occurred near the western side of the Mw 7.5 rupture zone.

We conducted MT surveys to elucidate the structural characteristics of the swarm activity and to determine whether there were structural differences from the area of the 2007 Noto Peninsula earthquake. The resistivity structure inverted from the onshore broadband electromagnetic field data acquired in 2021 and 2022 shows the existence of a continuous low-resistivity zone from the depth of the southern cluster, where a series of seismic swarms started, to the northern cluster, which is the upper extension of the source of non-steady crustal deformation. Furthermore, the clustered seismic located along the upper outer edge of this low resistivity zone, strongly suggesting the involvement of fluid in this activity. Preliminary 3D inversion covering only the central part of the Mw 7.5 rupture zone indicates good agreement between high-slip regions on the fault plane and zones of high resistivity.

In this presentation, we will report on the resistivity structure of the entire northern part of the Noto Peninsula, including data from supplemental observations conducted in 2022, 2023 and 2024 at 12 seafloor sites and two land sites to obtain higher resolution of the subsurface structure, as well as previously acquired data from 26 sites in the northwestern part of Noto Peninsula in 2007 (Yoshimura et al., 2008), and we discuss its relationship with the recent sequence of seismic activity.

2024年1月1日、能登半島北部で Mw7.5の大規模地震が発生し、強震動と津波による被害が広範囲に及んだ。この地震発生に先立ち、非火山地域であるこの地域では、2020年末より群発地震活動と局所的な非定常地殻変動が継続していた。この群発地震活動は、2018年6月頃に端を発し、2021年9月16日には M5.1、2022年6月19日には M5.4、2023年5月5日には M6.5の地震が発生し、そして 2024年1月1日の Mw7.5の地震の発生に至った。 Mw7.5の破壊域の西側付近では、2007年にも Mw6.7の地震が発生している。

我々は、群発活動が構造的にどのような場所で発生しているのか、また、2007年能登半島地震の発生域との構造的な違いを明らかにすることを目的として、地下比抵抗構造調査を実施してきた。2021~2022度に陸域で取得した計 55 か所の広帯域電磁場データに基づく解析からは、一連の群発活動が開始した南側のクラスタの深部から非地震性地殻変動源の上部延長にあたる北側のクラスタにかけて連続する低比抵抗領域の存在が明らかとなった。さらに、群発地震活動はこの低比抵抗領域の上部外縁部に集中しており、流体の関与を強く示唆する結果が得られた。

本発表では、地下構造の高解像度化を目的に、2022~2024 年度に実施した海域 12 点・陸域 2 点での補充観測データに加え、2007 年に取得された能登半島北西部 26 点のデータ(Yoshimura et al., 2008)を統合し、能登半島北部全域の比抵抗構造について報告し、一連の地震活動との関係について議論する。

D会場: 11/25 AM2(11:05-12:35)

11:50~12:05:00

広帯域マグネトテルリック法探査による伊豆半島の比抵抗構造

#井上 智裕 $^{1,5)}$, 相澤 広記 $^{1)}$, 重松 弘道 $^{1)}$, 中村 謙佑 $^{1)}$, 本田 貴之 $^{1)}$, 平田 一聖 $^{1)}$, 生田 璃音 $^{1)}$, 田中 伸一 $^{2)}$, 渡邉 篤志 $^{2)}$, 秋山 峻寛 $^{2)}$, 藤田 親亮 $^{2)}$, 西本 太郎 $^{2)}$, 小山 崇夫 $^{2)}$, 中川 潤 $^{3)}$, 長岡 愛理 $^{3)}$, 宮町 凜太郎 $^{3)}$, 吉村 令慧 $^{3)}$, 吉澤 史尚 $^{4)}$, 森田 裕一 $^{4)}$

(1 九州大学, (2 東京大学, (3 京都大学, (4 防災科学技術研究所, (5 産業技術総合研究所

The resistivity structure of Izu peninsula inferred from broadband magnetotelluric surveys

#Tomohiro Inoue^{1,5)}, Koki Aizawa¹⁾, Hiromichi Shigematsu¹⁾, Kensuke Nakamura¹⁾, Takayuki Honda¹⁾, Issei Hirata¹⁾, Rion Ikuta¹⁾, Shinichi S. Tanaka²⁾, Atsushi Watanabe²⁾, Takahiro Akiyama²⁾, Chikaaki Fujita²⁾, Taro Nishimoto²⁾, Takao Koyama²⁾, Jun Nakagawa³⁾, Airi Nagaoka³⁾, Rintaro Miyamachi³⁾, Ryokei Yoshimura³⁾, Fumihisa Yoshizawa⁴⁾, Yuichi Morita⁴⁾

⁽¹Kyushu University, ⁽²The University of Tokyo, ⁽³Kyoto University, ⁽⁴National Research Institute for Earth Science and Disaster Resilience, ⁽⁵National Institute of Advanced Industrial Science and Technology

The Izu Peninsula is located at the northern end of the Izu – Bonin volcanic arc along the eastern margin of the Philippine Sea Plate, and is known as the region where the plate has collided with Honshu. Volcanic activity has continued in the Izu Peninsula from approximately 20 million years ago to the present, forming a group of monogenetic volcanoes known as the Higashi-Izu Monogenetic Volcano Group. In the coastal to offshore area of eastern Izu Peninsula, earthquake swarm reflecting magmatic activity occurred notably in 1930 and during the 1970s to 1990s, accompanied by ground inflation around the region. Their events imply the presence of magmatic activity beneath the Izu Peninsula. Furthermore, the northern part of the Izu Peninsula hosts the Tanna Fault, which generated the 1930 North Izu Earthquake. Therefore, it is necessary to clarify the interaction between magmatic and seismic activities. The subsurface structure of the Izu Peninsula remains unclear, and the relationship between magmatic and seismic activities has not been fully clarified. In this study, we conducted broadband magnetotelluric (BBMT) survey from January to March 2025.

We recorded time series data consisting of two horizontal electric and three magnetic field components by the ELOG-MT system (NT system design Co. Ltd.) at 15 measurement sites. At 17 sites, we measured two horizontal electric fields by the ELOG-1k system (NT system design Co. Ltd.) without magnetic components. We acquired time series data with 32 Hz sampling rates. High frequency bandwidth data were acquired with 1024 Hz sampling rates during one hour at night (UT: $17:00^{\circ}18:00$). We calculated the MT responses (impedance tensor and geomagnetic transfer function) from the time-series data using the TRACMT code (Usui et al., 2024, GJI) using horizontal magnetic field measured at Kuju area (about 750 km from the west of the survey area). We obtained relatively high-quality response functions over a wide frequency range. At 14 sites from the western to the central part, the Z_{xy} component shows the phases out of the quadrant (POQ) in the long-period band (approximately 50-4000 s).

We used the FEMTIC code (Usui, 2015, GJI; Usui et al., 2017, GJI; Usui et al., 2024) and estimated the resistivity structure that reproduces the observed POQ features using 3-D inversion. The error floors of the impedance tensor and the geomagnetic transfer function were set to 5 % (off-diagonal components) and 10 % (diagonal components) and 0.02, respectively. A uniform half-space of 100 Ω m was used for initial model, in which the resistivities of the blocks corresponding to sea and air were fixed at 0.33 and 10^8 Ω m, respectively. The inversion results revealed a conductive anomaly at a depth of 5 km in the northern Izu Peninsula, while a resistive zone appeared at approximately 15 km depth in the southern area. In this presentation, we will show the preliminary resistivity structure of the Izu Peninsula and discuss the detailed anomalies.

Acknowledgments

This study was funded by the "Integrated Program for NEXT Generation Volcano Research and Human Resource Development" of MEXT. This study was supported by ERI JURP 2024-F2-04 in Earthquake Research Institute, the University of Tokyo.

伊豆半島は、フィリピン海プレート東縁を縁取る伊豆・小笠原火山弧の北端に位置し、同プレートの北上に伴い本州に衝突した地域として知られている。伊豆半島ではおよそ 2000 万年前から現在に至るまで火山活動が起きており、伊豆東部火山群と呼ばれる独立単性火山群が形成されてきた。伊豆東部火山群が分布する伊豆半島東部の沿岸から沖合にかけての領域では、1930 年や 1970~1990 年代を中心にマグマ活動を反映した群発地震が起こり、その周辺では地盤の隆起も観測されている。このことから、伊豆半島の地下ではマグマの存在やその活動が示唆される。さらに、伊豆半島の北部には 1930 年北伊豆地震を引き起こした丹那断層が存在し、マグマ活動と地震活動の相互作用を解明する必要がある。しかしながら伊豆半島の地下構造は明らかでなく、マグマ活動と地震活動の相互関係は十分に解明されていない。そこで、伊豆半島の地下比抵抗構造を明らかにすることを目的として、2025 年冬季(1~3 月)に伊豆半島全域で広帯域マグネトテルリック(MT)法観測を行った。

広帯域 MT 法観測は、NT システム社製 ELOG-MT、ELOG-1k を用いて 32 Hz(連続)、1024 Hz(UT17:00~18:00) サンプリングで、電磁場 5 成分(15 点)、電場 2 成分(17 点)を測定した。観測点どうしの間隔は約 5 \sim 15 km であり、計測期間は 1 地点につき約 14 日から 30 日間である。時系列解析には、リモートリファレンス点に九重で計測している観測点を使用し、TRACMT(Usui et al., 2024, GJI) を適用した。

時系列解析の結果、短周期から長周期にかけて比較的高品質な応答関数を得ることができた。伊豆半島西部や中央部の観測点では、Zxy 成分の長周期側に位相が 90° を超えるデータ(異常位相)が現れている。広範囲にかけて出現した異常位相データの存在は、特徴的な大規模構造が存在することを示唆する。

得られた応答関数をもとに、FEMTIC コード(Usui, 2015, GJI; Usui et al., 2017, GJI; Usui et al., 2024)を使用して構造解析に取り組み、異常位相を説明できるモデルの推定を試みた。予察的なインバージョンでは、インピーダンスの非対角成分に 5%、対角成分に 10%、ティッパーに絶対誤差 0.05 を与えた。そして、四面体メッシュを用いて、海と地形を反映させた初期モデルを作成した。インバージョンの結果、伊豆半島の北部で深さ 5 km に低比抵抗異常体が現れ、南側には深さ約 15 km に高比抵抗域が現れた。本発表では、試行錯誤を重ねて、より最適な比抵抗構造モデルを推定し、この異常体の詳細について議論する。

謝辞:本研究は、文科省による次世代火山研究・人材育成総合プロジェクトと東京大学地震研究所共同利用(2024-F2-04)の支援を受けました。

D会場: 11/25 AM2 (11:05-12:35)

12:05~12:20:00

#相澤 広記 $^{1)}$, 松島 喜雄 $^{2)}$, 松永 康生 $^{3)}$, 小山 崇夫 $^{4)}$, 長谷 英彰 $^{5)}$, 上嶋 誠 $^{4)}$ $^{(1)}$ 九州大学, $^{(2)}$ 産業技術総合研究所, $^{(3)}$ 産業技術総合研究所, $^{(4)}$ 東京大学地震研究所, $^{(5)}$ 地熱技術開発株式会社

A Practical Approach for Estimating Temporal Resistivity Changes in Volcanoes Using Broadband Magnetotelluric Data

#Koki Aizawa¹⁾, Nobuo Matsushima²⁾, Yasuo Matsunaga³⁾, Takao KOYAMA⁴⁾, Hideaki HASE⁵⁾, Makoto UYESHIMA⁴⁾
⁽¹Institute of Seismology and Volcanology, Faculty of Science, Kyushu University, ⁽²Geological Survey of Japan, AIST, ⁽³Fukushima Renewable Energy Institute, AIST, ⁽⁴Earthquake Research Institute, University of Tokyo, ⁽⁵Geothermal Energy Research and Development

Broadband magnetotelluric (MT) surveys have been widely conducted on volcanoes worldwide, often revealing a shallow conductive layer underlain by a column-shaped conductor. While imaging resistivity structure is a common application of MT, detecting temporal resistivity changes is more challenging due to surficial distortion and limited repeated measurements. In this study, we show a practical approach for estimating temporal resistivity changes using broadband MT data from two volcanoes. The first case involves repeated MT observations at 26 sites on Iwo-yama, Kirishima volcanic complex (2015 – 2017 and 2024), where a small phreatic eruption occurred in April 2018. The second case uses five months of MT recording (February – June 2010) at six sites on Sakurajima volcano.

MT response functions were estimated from electric and magnetic field time series using remote-reference processing. The most significant temporal changes appeared in vertical magnetic transfer functions (VTFs), emphasizing the importance of measuring vertical geomagnetic fields for resistivity monitoring. Changes in the phase tensor (Caldwell et al., 2004) were also detected, indicating that these variations reflect subsurface resistivity changes rather than surficial distortion.

We estimated 3-D resistivity changes using the FEMTIC code on a hexahedral mesh (Usui, 2015, 2024), incorporating two VTF components, four phase tensor components, and four impedance tensor components as input data. Galvanic distortion on the 2×2 impedance tensor was also considered. Although impedance data are susceptible to distortion, they remain necessary for constraining resistivity values. Phase tensor data help improve constraints, particularly in shallow regions. In the first step of the inversion, we determined a reference resistivity structure and corresponding galvanic distortion parameters using reference datasets (Iwo-yama: 2015 – 2016; Sakurajima: entire observation period). In the second step, these reference models were used as initial models for subsequent inversions (Iwo-yama: 2024 data; Sakurajima: monthly averaged data), enabling estimation of temporal 3-D resistivity changes.

At Iwo-yama, we found a substantial decrease in resistivity from the surface to ~200 m depth, coinciding with the area of post-eruption geothermal activation. This change likely reflects mixing of high-temperature volcanic fluids with shallow groundwater. The clay-rich cap layer expanded in an ENE – WSW direction and evolved into a more bell-shaped structure, potentially enhancing fluid storage. In contrast, the uppermost part locally increased in resistivity, possibly due to capping degradation from heating or acidification. These changes suggest an elevated potential for larger-scale phreatic eruptions. Interpretation of the Sakurajima results is ongoing, with volatile-rich fluids from magma interacting with groundwater as a possible mechanism.

D会場: 11/25 AM2(11:05-12:35)

12:20~12:35:00

島弧火山の形成メカニズム解明に向けた沈み込み帯の電気比抵抗構造における不均 質性の比較(2)

#畑 真紀 ¹⁾, CALDWELL Grant²⁾, 上嶋 誠 ³⁾, CALDWELL Alex²⁾, 吉村 令慧 ¹⁾, 小川 康雄 ⁴⁾, BERTRAND Ted²⁾, BENNIE Stewart²⁾, HEISE Wiebke²⁾

(1) 京都大学防災研究所, (2) ニュージーランド地球科学研究所, (3) 東京大学地震研究所, (4) 東京科学大学

Comparison of Resistivity Heterogeneity in Subduction Zones to Clarify the Formation Mechanism of Island Arc Volcanoes (2)

#Maki HATA¹⁾, Grant CALDWELL²⁾, Makoto UYESHIMA³⁾, Alex CALDWELL²⁾, Ryokei YOSHIMURA¹⁾, Yasuo OGAWA⁴⁾, Ted BERTRAND²⁾, Stewart BENNIE²⁾, Wiebke HEISE²⁾

⁽¹Disaster Prevention Research Institute, Kyoto University, ⁽²Earth Sciences New Zealand, ⁽³Earthquake Research Institute, the University of Tokyo, ⁽⁴Institute of Integrated Research, Institute of Science Tokyo

In subduction zones, the movement and distribution of fluids brought into the Earth's interior by the subducting oceanic plate (slab) are crucial for driving igneous/volcanic activity and seismic events. As these fluids reach specific temperature-pressure conditions during the subducting process, they are released from the oceanic plate through a dehydration reaction. The released fluids in the mantle lead to partial melting of the mantle, resulting in the formation of magma sources for island arc volcanoes. This process establishes volcanic chains/regions (on island arcs) that align with depth contour lines of the subducting plate. On the other hand, some island arcs, such as the island of Kyushu in Japan and the North Island of New Zealand, exhibit non-volcanic regions devoid of active Quaternary volcanoes for approximately 100 km. It is not entirely understood why volcanic and non-volcanic regions form, or why volcanic chains are discontinuous in a single-island arc despite being under the same tectonic conditions. Thus, a key objective of our research is to obtain and compare subsurface heterogeneity information for different island arcs using the electromagnetic method to aid in understanding the mechanism behind the formation of island-arc volcanoes.

In addition, due to the subduction of oceanic plates, various types of earthquakes have recurrently occurred in and around the island of Kyushu and the North Island of New Zealand, including significant thrust earthquakes offshore and historic earthquakes along tectonic lines within the land area. We have constructed three-dimensional (3-D) electrical resistivity structures by inverting magnetotelluric (MT) data, which were collected across the entirety of Kyushu through various surveys, to elucidate the fluid/magma distribution beneath Kyushu [e.g., Hata et al., 2015; 2017; 2020]. The 3-D resistivity models reveal magma and fluid systems associated with slab-derived fluid as notable electrical resistivity features/anomalies. Furthermore, we conducted long-period MT surveys over a 300 km \times 150 km area, encompassing the southernmost part of the Taupo volcanic zone (TVZ) and a non-volcanic region on the North Island of New Zealand within the Hikurangi subduction zone, from July 2023 to January 2024. The primary objective of these surveys is to extract information on subsurface heterogeneity, covering the depths of the crust and mantle in the transition area between the TVZ and the non-volcanic region, as a 3-D electrical resistivity model. In this presentation, we provide a detailed discussion of the subsurface heterogeneity beneath the transition area between the volcanic and non-volcanic regions of the two island arcs, as inferred from the 3-D resistivity distribution.

ポスター3:11/26 PM2/PM3 (14:50-18:25)

LEMI 長周期 MT 観測装置の周波数特性の検定について

#上嶋 誠 $^{1)}$, 市來 雅啓 $^{2)}$, 畑 真紀 $^{3)}$, 海田 俊輝 $^{2)}$, 臼井 嘉哉 $^{1)}$, 渡部 熙 $^{1,4)}$, 小川 康雄 $^{5)}$, 北岡 紀広 $^{5)}$ (1 東京大学地震研究所, $^{(2}$ 東北大学, $^{(3}$ 京都大学防災研究所, $^{(4}$ 東京大学地震研究所, $^{(5)}$ 東京科学大学

Calibration of the LEMI long-period MT instruments

#Makoto Uyeshima¹⁾, Masahiro ICHIKI²⁾, Maki HATA³⁾, Toshiki Kaida²⁾, Yoshiya USUI¹⁾, Akira WATANABE^{1,4)}, Yasuo OGAWA⁵⁾, Norihiro KITAOKA⁵⁾

⁽¹Earthquake Research Institute, the University of Tokyo, ⁽²Tohoku University, ⁽³Disaster Prevention Research Institute, Kyoto University, ⁽⁴Earthquake Research Institute, the University of Tokyo, ⁽⁵Institute of Science Tokyo

The LEMI long-period magnetotelluric (MT) instrument measures 3 component magnetic field with a fluxgate sensor and 4 channel electrical potential differences. Due to low power consumption and good quality of the magnetic sensor against temperature drift, the instrument is widely used in the MT community in the world. We also used the instruments for surveys in several target areas such as Tohoku, Kii Peninsula, and North Island of the New Zealand. After estimating the MT impedance between the electric field and the magnetic field, however, we found anomalous behavior of impedance especially in the phase in the shorter period range (shorter than 100s). In many cases, the phase value decreases toward the shorter periods. Thus, unless we get the calibration table for the instruments, we cannot obtain the correct impedances and estimate the true resistivity structure. The manufacturer only gave us a single typical calibration table, where frequency characteristics, however, were somewhat differenct from channel to channel and not very reliable.

Thus it is very important to determine the calibration table for respective channels in the MT recorders of respective serial numbers. In order to realize this, we performed the parallel MT observation at Samegawa site in Fukushima prefecture. We install one wide-band MT system (ADU08e produced by Metronix) and four LEMIs in the field. ADU08e measured 2 component electric fields and 3 component magnetic fields by using induction coils at 32 Hz sampling rate. All the electric channels of all the LEMIs measured the electric field of EW component and respective LEMIs measures 3 component magnetic field with respective fluxgate sensors at 1 Hz sampling rate. We obtained the records for about two months from June to August, 2025.

We estimated the response functions in the period range from 4s to 10^4s between EW component electric fields obtained by respective LEMIs and the ADU08e. We also estimated the response functions between vertical components obtained by respective LEMIs and the ADU08e. In this estimation, we used the BIRRP code developed by Chave and Thomson (2004). For the electric field, the phase value starts to decrease from 100s and reaches about -150 degree at 4s. The minus sign indicates phase delay of LEMIs abainst the ADU. About the magnetic field we only estimate response functions between vertical component of respective LEMIs and that of ADU. In comparison with the electric field, the magnetic field response functions are not very stable and some scatters are detected. Moreover, we cannot estimate response functions for horizontal components since orientation of the sensors cannot be aligned. In spite of this difficulty, we found that magnetic field phase rotation is at most -15 degree throughout the period range. This result is consistent with our experience in MT impedance estimation mentioned above. But there exists some variation of the frequency characteristics from channel to channel and serial number to serial number. We realized that we have to do further efforts to obtain correct calibration table, especially for magnetic channels.

#Liu Yu¹⁾, Yu Peng¹⁾, Zhang Luolei¹⁾, Zhao Chongjin¹⁾, Huang Zuwei¹⁾ (1 同済大学

Magnetotelluric Probability Tomography Based on the Correlation between **Impedance Perturbations and the Fréchet Operators**

#Yu Liu¹⁾, Peng Yu¹⁾, Luolei Zhang¹⁾, Chongjin Zhao¹⁾, Zuwei Huang¹⁾ (1 Tongji University

Probability Tomography, which was initially proposed by Patella (1997), has been extensively applied across geophysical exploration fields. The method calculates a probability value for each subsurface node, which quantifies the likelihood of an anomalous source (e.g., a charge, dipole, or physical property contrast) existing at that location.

The magnetotelluric (MT) probability tomography (Mauriello, 1999) uses electromagnetic induction field components (Equations 1 and 2) to derive charge-occurrence probability for TM mode (Equation 3) and dipole-occurrence probability for TE mode (Equation 4), thereby enabling a rapid reconstruction of the probable geometry of anomalous bodies without costly iteration. Here, the terms $(x-x_n)/[(x-x_n)^2+z_n^2]$ and $-z_m/[(x-x_m)^2+z_m^2]$ represent the space domain electric and magnetic tomography scanners, respectively.

However, this MT probability tomography employs frequency-independent scanners, neglecting the differential contributions of subsurface structures to the surface frequency response. To overcome this drawback, we introduce a novel probability tomography approach founded on the correlation of impedance perturbations with the Fréchet operators, as derived from the first-order Taylor expansion of the MT impedance (Equation 5). Its core principle involves calculating the correlation between the field generated by a unit source at the subsurface node and the measured anomalous field. This advancement allows effective integration of multi-frequency data.

To implement this method, the subsurface region is discretized into Q elementary cells, each with constant resistivity. The background impedances are obtained through forward modeling of a reference model, while the Fréchet operators are computed using the adjoint-state method. Thus, the core probability function for this technique is defined by Equation 6, where L is the number of frequencies, N is the number of measuring points, and W_d is the data weight matrix, which balances the disparities across different frequencies and measurement errors.

The effectiveness of the proposed method has been validated through extensive synthetic model tests (Figure 1 is result of synthetic three-block model). The results demonstrate that our method can characterize the morphology, boundaries, and depth extent of anomalous bodies with remarkable computational efficiency. This approach effectively mitigates the inherent limitations of conventional probability tomography, particularly its insufficient ability to differentiate between the depth and the resistivity values of anomalous bodies. Integrating the probability distributions of the TE and TM modes with the reference model's allows for the construction of an initial model that more closely approximates the true geological structure. This provides reliable initial constraints for subsequent inversion, significantly enhancing its convergence speed and the reliability of the final model. In addition, we applied the method to a real dataset acquired from the Junggar Basin.

$$\mathbf{E}(\mathbf{r}) = \frac{1}{4\pi\varepsilon_0} \sum_{n=1}^{N} \frac{\Gamma_n(\mathbf{r} - \mathbf{r}_n)}{|\mathbf{r} - \mathbf{r}_n|^3} + \frac{\mu_0 \omega^2}{4\pi} \sum_{m=1}^{M} \frac{\mathbf{P}_m}{|\mathbf{r} - \mathbf{r}_m|}$$
(1)

$$\mathbf{H}(\mathbf{r}) = \frac{i\omega}{4\pi} \sum_{m=1}^{M} \nabla \times \frac{\mathbf{P}_{m}}{|\mathbf{r} - \mathbf{r}_{m}|}$$
 (2)

$$\eta_{x}^{E}(x_{n}, z_{n}) = \frac{\sqrt{z_{n}} \int_{-\infty}^{+\infty} E_{x}(x) \frac{x - x_{n}}{(x - x_{n})^{2} + z_{n}^{2}}}{\sqrt{\frac{\pi}{2}} \int_{-\infty}^{+\infty} E_{x}^{2}(x) dx}$$
(3)

$$\eta_x^H(x_m, z_m) = \frac{\sqrt{z_m} \int_{-\infty}^{+\infty} H_x(x) \frac{-z_m}{(x - x_m)^2 + z_m^2}}{\sqrt{\frac{\pi}{2}} \int_{-\infty}^{+\infty} H_x^2(x) dx}$$
(4)

$$\Delta \mathbf{Z}(l,n) = \mathbf{Z}(l,n) - \mathbf{Z}^{ref}(l,n) = \sum_{i=1}^{Q} \frac{\partial \mathbf{Z}^{ref}(l,n)}{\partial \rho} \Delta \rho_{q}$$
 (5)

$$\eta_{x}^{H}\left(x_{m}, z_{m}\right) = \frac{\sqrt{z_{m}} \int_{-\infty}^{\infty} H_{x}\left(x\right) \frac{-z_{m}}{\left(x - x_{m}\right)^{2} + z_{m}^{2}}}{\sqrt{\frac{\pi}{2}} \int_{-\infty}^{+\infty} H_{x}^{2}\left(x\right) dx} \qquad (4)$$

$$\Delta \mathbf{Z}(l, n) = \mathbf{Z}(l, n) - \mathbf{Z}^{ref}\left(l, n\right) = \sum_{q=1}^{D} \frac{\partial \mathbf{Z}^{ref}\left(l, n\right)}{\partial \rho_{q}} \Delta \rho_{q} \qquad (5)$$

$$\eta_{q} = \frac{\sum_{l=1}^{L} \sum_{n=1}^{N} W_{d}\left(l, n\right) \Delta \mathbf{Z}\left(l, n\right) \frac{\partial \mathbf{Z}^{ref}\left(l, n\right)}{\partial \rho_{q}}}{\sqrt{\sum_{l=1}^{L} \sum_{n=1}^{N} \left[W_{d}\left(l, n\right) \Delta \mathbf{Z}\left(l, n\right)\right]^{2} \cdot \sum_{l=1}^{L} \sum_{n=1}^{N} \left[\frac{\partial \mathbf{Z}^{ref}\left(l, n\right)}{\partial \rho_{q}}\right]^{2}}} \qquad (6)$$

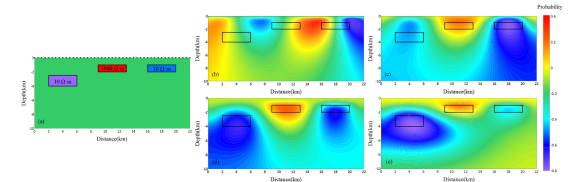


Figure 1. Comparison of imaging methods for the synthetic three-block model. (a) True model. (b) nventional TM-mode result (charge probability at 10Hz). (c) Conventional TE-mode result (dipole probability at 10Hz). (d) Proposed probability tomography (TM model). (e) Proposed probability tomography (TE model).

趙 崇進 $^{1)}$, #張 羅磊 $^{1)}$, 于 鵬 $^{1)}$, 黄 祖偉 $^{1)}$, 歌田 久司 $^{2)}$ $^{(1)}$ 同済大学, $^{(2)}$ 東京大学地震研究所

Reconciling Cartesian and Spherical Coordinate Approaches in Magnetotelluric Modeling: Source Conditions and Impedance Formulation

Chongjin Zhao¹⁾, #Luolei Zhang¹⁾, Peng Yu¹⁾, Zuwei Huang¹⁾, Hisashi UTADA²⁾
⁽¹Tongji University, ⁽²Earthquake Research Institute, The University of Tokyo

Since Cagniard (1953) first presented the basic theory of the magnetotelluric (MT) method, model calculations have traditionally been carried out in Cartesian coordinates, assuming plane-wave sources. However, because MT observations are made on the Earth, the fundamental theory and modeling tools should first be constructed in spherical coordinates, and the Cartesian framework, even if adopted for reasons of computational convenience, should be used only while maintaining consistency with the spherical-coordinate formulation.

In general, modeling in spherical coordinates employs an external dipole as the source. A set of three orthogonal external dipoles with unit amplitude is used as basis for representing arbitrary sources. The magnetic field generated by an external dipole has the simplest possible spatial structure (spatially uniform) that can physically exist. For a dipole oriented in the north – south direction, it is well known that the tangential component of the magnetic field at any point on the Earth's surface is proportional to the cosine of the latitude, while the radial component is proportional to the sine. This implies that assuming a plane-wave source in Cartesian coordinates represents a spatial structure even simpler than that of any external magnetic field that can exist in reality. At the very least, modeling with plane-wave sources in Cartesian coordinates cannot be regarded as consistent with modeling using dipole sources in spherical coordinates.

In this study, we approximately represent an external dipole source in spherical coordinates by finite-wavenumber sine/cosine functions in Cartesian coordinates, and investigate how deviations from the plane-wave assumption affect the impedance and tipper. Following Srivastava (1966), the source effect is expressed by approximating the wavenumber $\nu_n = \sqrt{(n(n+1))/a}$, which corresponds to a given spherical harmonic degree n. Using this framework, we systematically examined through numerical experiments the following four issues:

- (1)the appropriate treatment of the space above the Earth's surface in numerical models when the wavenumber is finite;
- (2)the lower bound of source harmonic degree (wavenumber) for which the plane-wave approximation holds;
- (3)the appropriate choice of a set of basis sources for representing an arbitrary source in a Cartesian coordinate system; and
 - (4)the uniqueness of impedance and tipper in the presence of source dimension effects.

The results show that:

- (1) when the wavenumber is nonzero, the conductivity values in the region above the Earth's surface have no significant influence on the calculation results; and
- (2)the lower bound of the source order for which the plane-wave approximation holds depends on frequency, and that within the frequency band relevant to MT observations, the plane-wave approximation is generally valid for external dipole sources.

For issues (3) and (4), no definitive conclusions have been reached at this stage, and further investigation is required.

#デウィ チナンチャ ニルマラ $^{1)}$, 吉村 令慧 $^{2)}$, 畑 真紀 $^{2)}$, 宮町 凜太郎 $^{2)}$, 小松 信太郎 $^{2)}$, 山崎 健一 $^{2)}$, 園田 忠臣 $^{2)}$, 竹中 悠亮 $^{2)}$

(1 京大 理学研究科, (2 京都大学防災研究所

Comparison of 1D and 2D Inversion Results of Magnetotelluric Data Acquired at Sakurajima Volcano

#Cinantya Nirmala Dewi¹⁾, Ryokei YOSHIMURA²⁾, Maki HATA²⁾, Rintaro Miyamachi²⁾, Shintaro Komatsu²⁾, Ken'ichi Yamazaki²⁾, Tadaomi Sonoda²⁾, Takenaka Yuusuke²⁾

(1 Graduate School of Science, Kyoto University, (2 Disaster Prevention Research Institute, Kyoto University

A total of 35 magnetotelluric (MT) soundings were carried out on Sakurajima Island in FY2024. The MT data cover a broadband frequency range from 0.001 to 400 Hz. After checking the data, we identified the artificial noise at approximately 60 Hz and 0.1 Hz. Therefore, the time series data were processed using the notch filter and remote reference method to reduce the noise. The magnetic data from Sukomo (SKM) and Noto (ONT-308) sites were used as a reference. As a preliminary step toward 3D inversion, this study aims to evaluate the ability of the 1D and 2D inversions to reveal the underground resistivity structure beneath the Sakurajima Volcano. The 1D analyses were carried out using Occam's inversion code (Constable et al., 1987) from the sum of squared (ssq; Rung-Arunwan et al., 2016) elements of the impedance tensor. Then, we performed the 2D inversions using the inversion code of Ogawa and Uchida (1996).

The almost similar underground resistivity structures are observed in both 1D and 2D models. Both the 1D and 2D results highlight three main resistivity structures that exist on Sakurajima Island. The near-surface resistive structure is correlated with the lava layer to prevent the upwelling volcanic flow. Then, the conductive structure was found in the NE-SW direction of Sakurajima Island. It seems to have a strong correlation with the magma plumbing system from Aira Caldera to the active crater. The 1D results indicate two conductive zone around Kitadake is separated by a high resistivity layer. However, in the 2D model, this conductive zone appears as a single conductive structure. The conductive structure was also found in the west of Sakurajima Island. In this area, the 2D results show a thin resistive layer near the surface and a conductive layer beneath it. Moreover, the 1D results also indicate the presence of a high-resistivity layer below the conductive zone. We suggest that this conductive zone represents the lateral intrusion of magma from the main NE-SW magma pathway, as proposed by Hidayati et al (2007). Then, the high resistivity structures were observed underlying the magma chamber beneath the Kitadake crater and on the southeastern side of Sakurajima Island, both in 1D and 2D models.

The above results show that 1D and 2D models can be used as an initial approach in structural imaging. Comparing 1D and 2D models leads us to gain valuable information about the main structure of Sakurajima. However, the 1D model does not take into account the distribution of land, sea, and 3D structure. Meanwhile, the 2D model is depend on the profile orientation on the structure. Therefore, we need to perform 3D inversion to obtain a more reliable model and compare it with 1D and 2D results to reveal the underground structure more comprehensively.

#渡部 熙 $^{1)}$, 上嶋 誠 $^{2)}$, 小川 康雄 $^{3)}$, 市來 雅啓 $^{4)}$, 山口 覚 $^{5)}$, 臼井 嘉哉 $^{6)}$, 村上 英記 $^{7)}$, 小河 勉 $^{1)}$, 大志万 直人 $^{7)}$, 吉村 令 慧 $^{8)}$, 相澤 広記 $^{9)}$, 塩崎 一郎 $^{10)}$, 笠谷 貴史 $^{11)}$

 $^{(1)}$ 東京大学地震研究所, $^{(2)}$ 東京大学地震研究所, $^{(3)}$ 東京科学大学, $^{(4)}$ 東北大学, $^{(5)}$ 東京大学地震研究所, $^{(6)}$ 東京大学地震研究所, $^{(6)}$ 東京大学地震研究所, $^{(7)}$ 京都大学防災研究所, $^{(8)}$ 京都大学防災研究所, $^{(9)}$ 九州大学地震火山観測研究センター, $^{(10)}$ 鳥取大学大学院, $^{(11)}$ 海洋研究開発機構

Analysis of the Network-MT and conventional MT data measured in the southern part of Kii Peninsula, Southwestern Japan

#Akira Watanabe¹⁾, Makoto UYESHIMA²⁾, Yasuo OGAWA³⁾, Masahiro ICHIKI⁴⁾, Satoru YAMAGUCHI⁵⁾, Yoshiya USUI⁶⁾, Hideki MURAKAMI⁷⁾, Tsutomu OGAWA¹⁾, Naoto Oshiman⁷⁾, Ryokei YOSHIMURA⁸⁾, Koki AIZAWA⁹⁾, Ichiro SHIOZAKI¹⁰⁾, Takafumi KASAYA¹¹⁾

⁽¹Earthquake Research Institute, University of Tokyo, ⁽²Earthquake Research Institute, University of Tokyo, ⁽³Institute of Science Tokyo, ⁽⁴Tohoku university, ⁽⁵Earthquake Research Institute, University of Tokyo, ⁽⁶Earthquake Research Institute, University of Tokyo, ⁽⁷Disaster Prevention Research Institute, ⁽⁸Disaster Prevention Research Institute, ⁽⁹Institute of Seismology and Volcanology, Kyushu University, ⁽¹⁰Tottori University, ⁽¹¹JAMSTEC

The Kii Peninsula in the forearc region of southwestern Japan has distinct structural and tectonic features due to the subducting Philippine Sea (PHS) slab. These features include high seismicity, deep low-frequency earthquakes (DLEQ), and hot springs containing high 3He/4He isotopic ratios. These tectonic and geological activities may be caused by interstitial fluids released from the subducting PHS slab. Since electrical resistivity is one of the physical properties sensitive to the existence and connectivity of subsurface fluids, elucidating its structure beneath the Kii Peninsula is key to understanding the relationship between deep fluids and various tectonic activities. In this study, we analyzed long-period MT data, wide-band MT data, and network-MT data acquired in the Kii Peninsula to obtain a 3-D deep resistivity structure of higher resolution and accuracy in the vicinity of the DLEQ source area.

The network-MT (NMT) method employs a commercial telephone network to obtain voltage difference data over long lengths. We obtain better data than conventional MT methods in the following points: higher signal-to-noise ratio, less static effects, and easier acquisition of long-period data. Therefore, the NMT data enable us to resolve conductivity structure in deeper areas than the conventional MT method. On the other hand, it had low resolution for the middle and upper crust due to lack of high-frequency data. Additionally, observations can only be performed in areas where telephone lines are available. These two factors create gaps in data in both the spatial and frequency domains. To address these limitations, we are now trying to use and newly obtain conventional MT data from the wide-band and the long-period MT surveys and combined them with the Network-MT data.

In this presentation, we will present a basic characteristic of the so far obtained conventional MT data in the southern part of Kii Peninsula and compare them with the Network-MT data. We then discuss on an inversion scheme to combine both data sets, and present a preliminary 3-D resistivity structure by combining both data sets.

#黄 祖偉 $^{1)}$, 小山 崇夫 $^{2)}$, 于 鵬 $^{1)}$, 臼井 嘉哉 $^{2)}$ (1 同済大学, $^{(2)}$ 東京大学地震研究所

Forward Modeling Study of Controlled-Source Electromagnetic Based on the FEMTIC Program

#Zuwei Huang¹⁾, Takao KOYAMA²⁾, Peng Yu¹⁾, Yoshiya USUI²⁾
⁽¹Tongji University, ⁽²Earthquake Research Institute, The University of Tokyo

The Controlled-Source Electromagnetic (CSEM) method is a geophysical technique that uses an artificial electromagnetic source to investigate subsurface electrical conductivity variations. It operates in both marine and land environments and is particularly effective in inverting shallow targets, especially thin resistors compared to magnetotelluric (MT). In CSEM surveys, a known time-varying current—often from grounded electric dipole or current wire, which is injected into the Earth or ocean, generating primary electromagnetic (EM) fields. These primary fields interact with subsurface conductivity structures, inducing secondary electric currents whose associated EM fields can be measured at the surface or seafloor.

Forward modelling predicts the EM response for a given conductivity model and survey configuration, forming the foundation for interpretation and inversion. In realistic 3D geological settings, Maxwell's equations cannot be solved analytically, necessitating numerical approaches such as finite-element (FE), finite-difference (FD), finite-volume (FV), or integral-equation (IE) methods. In this study, we conduct forward modeling research on CSEM based on the open-source edge-based FE method MT program FEMTIC (Usui, 2015, 2017, 2021). The FEMTIC is particularly powerful for CSEM modelling because it can handle arbitrarily complex geometries through unstructured tetrahedral meshes. In the frequency domain, the Helmholtz equation for the electric field can be solved directly using edge-element basis functions, which ensure tangential field continuity. The FE approach involves discretizing the computational domain into tetrahedral elements, applying the Galerkin weighted-residual formulation, and assembling a sparse linear system representing the governing equations.

We use the total field equation as the governing equation for CSEM. Unlike the scattered field (secondary field) equation, the advantage of the total field equation is that it does not require the additional calculation of background electric field values. Its electric and magnetic field derivative matrices are consistent with those of MT (Since the source term is independent of the subsurface model conductivity), eliminating the need for further modifications. At the same time, it can better simulate field sources of arbitrary shapes. Correspondingly, to avoid computational singularities, we need to refine the mesh near the source to ensure the accuracy of the field source integration terms. We employ an accurate equivalent source method to discretize arbitrarily shaped sources. Unlike approaches that map current lines onto the edges of grid cells, our method identifies the actual contact relationship between the real field source and the grid elements. This allows us to determine the length, coordinates, and orientation of each wire segment passing through a certain grid cell, thereby enabling the simulation of arbitrarily shaped wires. In the program, we provide three types of field sources: (1) infinitesimally small magnetic dipole source with arbitrary orientation; (2) infinitesimally small electric dipole source with arbitrary orientation, (3) arbitrarily shaped wire (simulated using a polyline composed of multiple segments). By using the pseudo-Dirac function, we parameterize the field source. Leveraging the integral properties of the Dirac function, we achieve the calculation of the source integration term on the right-hand side of the governing equation. After incorporating the source term integration, by setting all outer boundary conditions in the CSEM simulation to the Dirichlet zero boundary condition, the forward modeling of CSEM can be achieved.

After modifying the CSEM forward modeling equations, we designed numerical experiments to demonstrate the accuracy of the CSEM forward modeling based on FEMTIC. The subsurface medium was modeled as a homogeneous half-space with a resistivity of $100~\Omega \cdot m$. Sixty observation points were evenly spaced along the y-axis at 150~m intervals in the east – west direction. The source was positioned at the center of the model (origin of the coordinate system), implemented as both a $1~A \cdot m$ moment electric dipole and a 1~m long current-carrying wire with a current of 1~A, both oriented in the due north direction. The analytical solution was computed using Dipole1D (Key, 2009). By comparing the CSEM results simulated with FEMTIC to the 1D analytical solutions, the average errors were found to be less than 1%, demonstrating the accuracy of the CSEM forward modeling based on FEMTIC. This lays a solid foundation for the subsequent development of the CSEM inversion module.

ポスター3:11/26 PM2/PM3 (14:50-18:25)

DEEPMAYMT:マヨット沖海底火山系の海底電磁気探査

#松野 哲男 $^{1)}$, 島 伸和 $^{1,2)}$, Wawrzyniak Pierre $^{3)}$, D'Eu Jean-François $^{4)}$, 杉岡 裕子 $^{1,2)}$, Tarits Pascal $^{4,5)}$, 土井 晴貴 $^{1)}$, 佐野 守 $^{1)}$

⁽¹⁾ 神戸大学 海洋底探査センター, ⁽²⁾ 神戸大学 理学部惑星学科, ⁽³⁾BRGM, Bureau des Recherches Géologiques et Minières, ⁽⁴⁾MAPPEM Geophysics SAS, ⁽⁵⁾IUEM, Institut Universitaire Européen de la Mer

DEEPMAYMT: Marine magnetotelluric investigation for a submarine volcanic system offshore Mayotte

#Tetsuo Matsuno¹⁾, Nobukazu Seama^{1,2)}, Pierre Wawrzyniak³⁾, Jean-François D'Eu⁴⁾, Hiroko Sugioka^{1,2)}, Pascal Tarits^{4,5)}, Haruki Doi¹⁾, Mamoru Sano¹⁾

⁽¹Kobe Ocean-Bottom Exploration Center, Kobe University, ⁽²Department of Planetology, Kobe University, ⁽³BRGM, Bureau des Recherches Géologiques et Minières, ⁽⁴MAPPEM Geophysics SAS, ⁽⁵IUEM, Institut Universitaire Européen de la Mer

Mayotte, located in the Comoros Archipelago within the Mozambique Channel, has experienced significant seismic activity that began abruptly in May 2018. Subsequent investigations identified the formation of a new large submarine volcanic edifice, Fani Maoré, approximately 50 km east of Mayotte, and revealed associated seismic activity, crustal deformation, and petrological and geochemical signals linked to this volcanic event (e.g., Feuillet et al., 2021). Two seismically active zones have been identified offshore Mayotte: one located approximately 10-20 km east of the island, and the other situated between this first zone and Fani Maoré. The former zone exhibits a seismic swarm at depths of ~20-45 km, overlain by very low-frequency events, and is associated with volcanic processes such as fault movements and gas emissions driven by two magma reservoirs. The latter zone includes another seismic swarm at depths of ~30-45 km and shallower earthquakes trending toward Fani Maoré, which are interpreted as reflecting a magma supply pathway to the edifice.

The French Geological Survey (BRGM) has initiated electromagnetic surveys to investigate this volcanic system and monitor its activity. Results from land-based and shallow-marine electromagnetic data have revealed a conductive layer below ~15 km depth beneath Petite Terre of Mayotte, as well as a conductor at 5-13 km depth offshore to the east of Petite Terre (Darnet et al., 2020). To further characterize the electrical resistivity structure of the volcanic system in deeper offshore regions, BRGM and Kobe University launched a deep marine magnetotelluric experiment near Mayotte. In October 2024, we deployed seven Ocean-Bottom Electro-Magnetometers (OBEMs) from Kobe University and successfully recovered all instruments in March 2025. The OBEMs were installed at depths of 740-1870 m to widely cover the primary seismic zone, while avoiding rough bathymetric areas caused by slopes and volcanic topography, based on detailed bathymetric data reviewed in advance. The instruments recorded time variations of the electromagnetic field, as well as tilt and temperature at the seafloor, at sampling rates of 8 Hz for approximately two to four weeks, followed by 60 s intervals until the end of the measurement. We are currently processing the time-series data and estimating magnetotelluric response functions for subsequent 3-D inversion of the electrical resistivity structure. In December 2024, Cyclone "Chido", which is the most powerful storm to strike Mayotte on record, impacted the region. The OBEM data may therefore contain electromagnetic signals generated by the cyclone.

モザンビーク海峡に位置するコモロ諸島のマヨットでは、2018 年 5 月に突如開始した顕著な地震活動が観測された。その後の調査により、マヨットの東約 50 km に新たな大規模海底火山体「ファニ・マオレ (Fani Maoré)」が形成されたことが確認され、この火山活動に関連する地震活動、地殻変動、岩石学的・地球化学的なシグナルが明らかになっている(Feuillet et al., 2021 など)。マヨット沖では、2 つの地震活動域が特定されている。1 つは島の東約 10-20 km に位置し、もう 1 つはこの最初の領域とファニ・マオレの間にある。前者は深さ約 20-45 km に見られる地震発生域と、その上方の超低周波地震域であり、これらは、2 つのマグマ溜まりに起因する断層運動やガス放出などの火山プロセスと関連していると考えられている。後者は深さ約 30-45 km の別の地震発生域と、そこからファニ・マオレに向かう経路で発生する浅部地震であり、これらは、火山体へのマグマ供給経路を反映すると解釈されている。

フランス地質調査所(BRGM)は、この火山系を調査し、その活動を監視するために電磁気探査を開始した。陸上および浅海域の電磁気データから、マヨットのプチ・テール下の深さ約 15 km 以深に低比抵抗層が存在すること、さらにプチ・テール東方沖の深さ 5-13 km に低比抵抗体が存在することが明らかになっている(Darnet et al., 2020)。この火山系の深部海域における比抵抗構造をさらに詳細に把握するため、BRGM と神戸大学はマヨット沖で海底電磁気探査を行った。2024 年 10 月に神戸大学の海底電位差磁力計(OBEM)7 台を設置し、2025 年 3 月に全ての機器を回収した。OBEM は、水深 740-1870 m の上記第 1 の地震活動域を広くカバーする範囲に設置した。斜面や火山地形による複雑な海底地形を避けるため、事前に詳細な海底地形データを確認した上で設置を行った。OBEM は海底での電磁場の時間変化に加え、機器傾斜と温度を記録し、最初の 2-4 週間は 8 Hz で、その後は 60 秒間隔で測定を行った。現在、時系列データを処理し、3 次元比抵抗構造推定インバージョンに向けて電磁応答関数を推定している。なお、2024 年 12 月には、観測記録上最強のサイクロン「チド」がマヨット地域に襲来した。そのため、OBEM データにはサイクロンによる電磁波シグナルが含まれている可能性がある。

#小畑 拓実 $^{1)}$, 松野 哲男 $^{2)}$, 南 拓人 $^{1)}$, 市原 寛 $^{3)}$, 臼井 嘉哉 $^{4)}$, 巽 好幸 $^{2)}$, 杉岡 裕子 $^{1,2)}$, 大塚 宏徳 $^{4)}$, 島 伸和 $^{1,2)}$ $^{(1)}$ 神戸大学・理・惑星、 $^{(2)}$ 神戸大学・海洋底探査センター、 $^{(3)}$ 名古屋大学・地震火山研究センター、 $^{(4)}$ 東京大学・地震研究所

Resistivity structure beneath the Kikai submarine caldera volcano and tidally induced EM signals from OBEM observations

#Takumi OBATA¹⁾, Tetsuo MATSUNO²⁾, Takuto MINAMI¹⁾, Hiroshi ICHIHARA³⁾, Yoshiya USUI⁴⁾, Yoshiaki TATSUMI²⁾, Hiroko SUGIOKA^{1,2)}, Hironori OTSUKA⁴⁾, Nobukazu SEAMA^{1,2)}

⁽¹Department of Planetology, Graduate School of Science, Kobe University, ⁽²Kobe Ocean Bottom Exploration Center, Kobe University, ⁽³Earthquake and Volcano Research Center, Graduate School of Environmental Studies, Nagoya University, ⁽⁴Earthquake Research Institute, the University of Tokyo

This study aims to understand the current magma supply system that could lead to giant caldera-forming eruptions. The Kikai submarine caldera volcano, located in southern Kagoshima Prefecture, is known for the 7.3 ka caldera-forming eruption, the most recent giant caldera eruption in Japan. Topographic and petrological studies indicate that a central lava dome was emplaced by renewed magma supply after this eruption (Tatsumi et al., 2018). To investigate the current state of the magma supply system, we deployed and recovered 32 Ocean Bottom Electro-Magnetometers (OBEMs) around the Kikai Caldera between 2016 and 2022. In this presentation, we report (1) improvements in the estimation of the resistivity structure using MT surveys, and (2) characteristics of the observed data in the tidal frequency band.

- (1) Sub-seafloor resistivity structures inferred from the present dataset have previously been reported (Obata et al., 2025, JpGU). Here, we present an improved resistivity model obtained through a three-step inversion procedure, including one-dimensional structure estimation using the Occam 1D method (Constable et al., 1987).
- (2) Tidally induced magnetic variations arise as conductive seawater moves in the geomagnetic main field, and these signals can be observed both by satellites and at the seafloor. Inversions using satellite data have already been conducted (Grayver et al., 2016, 2017). Seafloor observations, however, provide access to toroidal magnetic fields that cannot be detected at satellite altitudes, thus potentially placing new constraints on resistivity modeling. From the OBEM data obtained in this study, vertical electric fields could be estimated by calculating potential differences among multiple electrodes. We present characteristics of the magnetic field data in the tidal frequency range, as well as observations of vertical electric field.

ポスター3:11/26 PM2/PM3 (14:50-18:25)

3次元磁重力逆解析における Total Variation 正則化手法の構造ガイド法を用いた改善

#宇津木 充 ¹⁾ (1 京都大学

Improvement of the total variation regularization of the 3D magnetic and gravity inversion using the structural guide method

#Utsugi Mitsuru¹⁾

(1 Kyoto University, Institute for Geothermal Sciences

In structural analysis using magnetic and gravity anomaly data, regularization is essential because the problem is underdetermined. In addition to the classical L2 norm regularization method, various techniques, including sparse regularization methods such as the L1 norm, Lp norm, and minimum support etc., have been proposed and studied. However, these methods commonly fail to effectively detect sharp boundaries, such as faults or structural boundaries. To address this, total variation (TV) regularization have been proposed(e.g., Bertete-Aguirre et al., 2002; Farquarson, 2008; Vatankhah et al., 2018; Utsugi, 2021). This method incorporates the spatial derivative vector of the structural model into the penalty term. The goal is to minimize the areas where the derivative is non-zero, which facilitates the emergence of models with block structures and improves the boundary representation capability of the resulting models. However, this method tends to produce elongated blocks along the derivative axis. For instance, when x-, y-, and z-axis derivatives are used for TV, the resulting model tends to exhibit blocks with surfaces along these axes. This can lead to failures in reproducing structures such as tilted slabs. To overcome this, it is common practice to assign weights to each derivative operator in each direction; however, the method of distributing these weights is often ad hoc and lacks generalization. In this study, we propose a method that uses information from other geophysical surveys as the structural guide. In this method, the weights of each differential operator are adjusted based on the available information about the subsurface structure. Synthetic tests confirmed that, when information about the shape of the subsurface structure is available, the reproduction capability, including the dipping slab, is greatly improved. However, this method cannot be used when detailed information about the subsurface structure is unavailable. As an alternative, we propose using models obtained from existing analysis methods as guides. In this presentation, we introduce an improved analysis method that uses models obtained through L1-L2 norm regularization inversion, as proposed by Utsugi (2019). Specifically, we present an enhanced version of L1-TV inversion method (Utsugi, 2021) that incorporates this approach.

磁重力データを用いた構造解析においては、解くべき問題が劣決定系であることから正則化を施すことが必須である。 そのため、L2 ノルム正則のような古典的な方法のほかにも、L1 ノルム、Lp ノルムや minimum support のスパース正則 など、様々な手法が提案され研究されている。しかしこれらに共通する欠点として、断層や構造境界などのシャープな境 界の検出が不得意であるという事が挙げられる。こうした境界検出、または境界を強調した構造モデルを得ることを目的 にした正則化手法として Total Variation(TV) が挙げられ、これを用いたインバージョンスキームも提案されている(e.g. Bertete-Aguirre et al. 2002; Farquarson 2008; Vatankhah et al 2018, Utsugi 2021)。これは構造モデルの空間微分ベクトル をペナルティに組み込んだもので、そのペナルティを最小化することで微分が非ゼロになる領域を最小化し、ブロック構 造を持つモデルを出現しやすくする。その結果、得られるモデルの境界表現能を向上させることを意図したものである。 しかしこの手法の欠点としては微分軸方向に伸びたブロックが得られやすいという事である。例えば TV として x,y,z 軸 方向の微分を用いた場合、得られるモデルは x,y,z 軸方向に面を持つブロックが現れやすく、その結果傾いたスラブのよ うな構造の再現に失敗する。この欠点を克服するために、各軸方向の微分オペレータに重みをつけることが一般に行われ るが、その重みの分配方法は場当たり的で一般化されていないことが多い。本研究では、この各微分オペレータの重みと して、他の物理探査などで得られた既存情報を用いた構造ガイド法を提案する。合成テストから、地下構造の形状につい ての情報がある場合にはその傾斜も含め再現能力が大幅に改善されることが確かめられた。但し地下構造について詳細 な情報が無い場合にはこの方法は利用できない。そこで代替え手法として、既存の解析手法で得られたモデルをガイドと して用いることを提案した。本発表では Utsugi(2019) で提案された L1-L2 ノルム正則化インバージョンにより得られた モデルをガイドとして用いるよう L1-TV1(Utsugi,2021) を改良した解析方法を紹介する。

ポスター3:11/26 PM2/PM3 (14:50-18:25)

ドローン電磁探査システムのプロトタイプ開発

#石須 慶一 $^{1)}$, 北岡 紀広 $^{2)}$, 小川 康雄 $^{2)}$, 寺田 暁彦 $^{2)}$ $^{(1)}$ 九州大学, $^{(2)}$ 東京科学大学

Development of a UAV-based Electromagnetic Exploration System Prototype

#Keiichi Ishizu¹⁾, Norihiro Kitaoka²⁾, Yasuo Ogawa²⁾, Akihiko Terada²⁾ (¹Kyushu university, (²Institute of Science Tokyo

Electromagnetic surveys in volcanic regions have traditionally faced the challenge of limited observation coverage due to the difficulty of accessing many areas on foot. As a solution, the semi-airborne electromagnetic (EM) method, which uses a ground-based transmitter and an airborne receiver, has garnered attention. However, conventional single-direction transmission has limitations in accurately estimating complex three-dimensional (3D) resistivity structures. Therefore, this research aimed to develop a prototype for a new semi-airborne EM survey system that utilizes two-directional transmister dipoles (tensor-type transmission) to improve the estimation accuracy of 3D structures from multi-directional transmission data. This system applies an electromagnetic cross-talk technique, simultaneously transmitting signals at slightly different frequencies from the two transmitter dipoles. This enables a single receiver mounted on a drone to separate and measure the signals from both transmitters simultaneously without interference. A custom receiver coil was built using a flat cable to create an observation system that could be mounted on a drone. To verify the performance of the developed system, a field experiment was conducted at the former Ishizu mine site, south of Mt. Kusatsu-Shirane. The results confirmed that the drone in flight could simultaneously measure the signals from the two ground-based transmitters as intended, thus demonstrating the fundamental performance of this system. The ability to acquire two-directional transmission data in a single flight is a unique strength that significantly improves survey efficiency. Future work will focus on further verifying the effectiveness of this system and aiming for its application in active volcanic regions.

#星野 咲華 $^{1)}$, 南 拓人 $^{1)}$, 原田 裕己 $^{2)}$, 寺田 直樹 $^{3)}$, 佐藤 雅彦 $^{4)}$, 小川 康雄 $^{3)}$, 松島 政貴 $^{5)}$, 清水 久芳 $^{6)}$, 野口 里奈 $^{7)}$ $^{(1)}$ 神戸大学, $^{(2)}$ 京都大学, $^{(3)}$ 東北大学, $^{(4)}$ 東京理科大学, $^{(5)}$ 東京科学大学, $^{(6)}$ 東京大学, $^{(7)}$ 新潟大学

Induction Vector Analysis of InSight Magnetic Data to Constrain Martian Mantle Structure

#Sakika Hoshino¹⁾, Takuto Minami¹⁾, Yuki Harada²⁾, Naoki Terada³⁾, Masahiko Sato⁴⁾, Yasuo Ogawa³⁾, Masaki Matsushima⁵⁾, Hisayoshi Shimizu⁶⁾, Rina Noguchi⁷⁾

⁽¹Kobe University, ⁽²Kyoto University, ⁽³Tohoku University, ⁽⁴Tokyo University of Science, ⁽⁵Institute of Science Tokyo, ⁽⁶University of Tokyo, ⁽⁷Niigata University)</sup>

Recent discoveries have challenged the long-held view that Mars has been geologically dormant since the Amazonian period. While Mars experienced intense volcanism and tectonics before and during the Hesperian period (~3.5 - 3.2 Ga), the Amazonian period (<3.2 Ga) has been characterized by relative inactivity with only limited volcanism. However, Horvath et al. (2021) identified young volcanic deposits in the Cerberus Fossae region of Elysium Planitia, suggesting eruptions occurred as recently as 210 to 50 ka. Broquet and Andrews-Hanna (2022) further demonstrated that such recent volcanic activity cannot be explained by conventional passive mechanisms, and instead proposed a geophysical low-density anomaly model of an active mantle plume beneath Elysium Planitia, supported by integrated analyses of gravity and topography. Nevertheless, substantial uncertainty remains regarding the detailed properties of the plume head, including its diameter (3,600 - 4,000 km), depth (25 - 200 km), and thickness (200 - 500 km). Additional constraints on the plume head properties are necessary and important for advancing our understanding of Martian interior dynamics.

To further constrain the shape and properties of the mantle plume in this region, we analyzed nightside magnetic field data from NASA's InSight lander, located on the inner side of the western boundary of the proposed plume head. We observed a systematic anti-clockwise rotation in the real part of induction vectors—from southeast to northeast—across periods ranging from 500 to 10,000 seconds. These vectors, expressed as (-Tx, -Ty) from the relationship $Bz = Tx \cdot Bx + Ty \cdot By$, point toward regions of anomalously low resistivity. Therefore, this result suggests the presence of a localized conductive anomaly several hundred kilometers beneath the eastern side of the InSight landing site, consistent with the influence of the proposed mantle plume.

To quantitatively interpret the result above, we conducted numerical simulations using the edge-based finite element method (Minami et al., 2018), incorporating Martian real topographic data. We tested a range of low-resistivity anomaly models with horizontally rectangular geometries and uniform thicknesses to evaluate their consistency with the observed induction vector behavior. Preliminary results indicate that the anomaly's western edge lies east of the InSight landing site, with its northern boundary extending further north and its southern edge located just a few hundred kilometers to the south. These findings support the mantle plume hypothesis and suggest that its structure may be more complex than a simple cylindrical form. Our study demonstrates the effectiveness of magnetic sounding techniques in revealing subsurface mantle structures and constraining the thermal and structural evolution of Mars.

ポスター3:11/26 PM2/PM3 (14:50-18:25)

2022 年 1 月 Hunga Tonga-Hunga Ha'apai 火山噴火後にアテーレおよびアピアで観測された 2 時間スケール磁場変動

#清水 久芳 ¹⁾

(1 東京大学地震研究所

Magnetic field variations with a 2-h timescale in Tonga and Samoa following the HTHH volcanic eruption on January 15, 2022

#Hisayoshi Shimizu¹⁾

(1 Earthquake Research Institute, University of Tokyo

The massive eruption of the Hunga Tonga-Hunga Ha'apai (HTHH) volcano on January 15, 2022, triggered a variety of phenomena, including intense lightning from plume activities, Lamb waves propagating through the atmosphere, conventional tsunamis alongside those influenced by Lamb waves, and TEC (total electron content) variations in the ionosphere. This presentation explores magnetic field variations with a timescale of approximately two hours following the eruption. These variations were most prominent in the vertical magnetic component observed at 'Atele (Tonga). Additionally, similar variations in the eastward magnetic component were detected at both 'Atele and Apia (Samoa). Simple electric current models in the ionosphere fail to adequately explain the magnetic field features observed at 'Atele and Apia simultaneously, if these variations were linked to localized electric current induced by the volcanic eruption in the ionosphere. This raises the possibility that the two-hour timescale variation observed at Apia was generated by an electric current of larger spatial scale and may not have been directly related with the eruption. Furthermore, it is emphasized that analyzing the vertical magnetic component with considerations of electromagnetic induction within the Earth is crucial for understanding the electric currents responsible for these magnetic field variations.

フレンチポリネシアの海底磁場データを用いたデータ同化による津波波高予測

#平野 喬之 $^{1)}$, 南 拓人 $^{1)}$, Saynisch-Wagner Jan $^{2)}$, Hornschild Aaron $^{2)}$, 林 智恒 $^{3)}$, 馬場 俊孝 $^{4)}$, 藤 浩明 $^{5)}$ (1 神戸大学, $^{(2)}$ GFZ ヘルムホルツ地球科学研究センター, $^{(3)}$ 統計数理研究所, $^{(4)}$ 徳島大学, $^{(5)}$ 京都大学

Tsunami wave height prediction using data assimilation of seafloor magnetic data in French Polynesia

#Takayuki HIRANO¹⁾, Takuto MINAMI¹⁾, Jan Saynisch-Wagner²⁾, Aaron Hornschild²⁾, Zhiheng Lin³⁾, Toshitaka BABA⁴⁾, Hiroaki TOH⁵⁾

⁽¹Kobe University, ⁽²GFZ Helmholtz Centre for Geosciences, ⁽³The Institute of Statistical Mathematics, ⁽⁴Tokushima University, ⁽⁵Kyoto University)</sup>

When electrically conductive seawater flows through Earth's geomagnetic field during tsunami propagation, interactions between the flow and the field generate secondary (induced) magnetic fields. These tsunami-generated magnetic (TGM) fields have been observed on the seafloor (Toh et al., 2011; Suetsugu et al., 2012), and theory and observations have advanced the understanding of TGM (e.g., Tyler, 2005; Minami et al., 2015, 2021). Unlike pressure data, TGM field allows estimation of propagation direction from single-point three-component measurements (Sugioka et al., 2014; Lin, 2024).

Data assimilation (DA) is a powerful tool that integrates observations with numerical simulations and has been widely used in weather forecasting. Recent studies have demonstrated its application to tsunami forecasting using linear long-wave models and pressure data (Maeda et al., 2015). However, previous tsunami DA studies have primarily used linear models and pressure data; there have been no prior reports that assimilate seafloor TGM data or that explicitly account for nonlinear effects, which intensify in shallow water.

This study implements DA that accounts for tsunami nonlinearity and assesses the utility of TGM fields by assimilating seafloor magnetic observations to predict the regional tsunami field in French Polynesia during the 2010 Chile earthquake tsunami. During the event, nine ocean-bottom electromagnetometers (OBEMs) and one differential pressure gauge (DPG) installed by TIARES recorded magnetic and pressure signals (Suetsugu et al., 2012; Sugioka et al., 2014). Strong nonlinear effects associated with complex archipelagic bathymetry have produced discrepancies between simulations and DPG records in arrival time and amplitude (Lin et al., 2021). Because TGM field provides propagation-direction information via single-point three-component measurements, it has the potential to improve prediction efficiency and accuracy compared with pressure alone.

We adopt the four-dimensional ensemble variational (4DEnVar) approach (Liu et al., 2008), which couples a forward model with sparse observations without tangent-linear/adjoint models and, under the assumption of weak nonlinearity, enables ensemble-based background error estimation and iterative updates.

To balance efficiency and physics (dispersion and nonlinearity), we employ a two-domain, two-step strategy: a compact target domain is embedded in a larger-scale domain. In the first step, we perform 44 dispersion-enabled JAGURS simulations (Baba et al., 2017) with unit slip on each subfault of the 2010 source model (Yoshimoto et al., 2016) and precompute Green's functions that map unit slip to time series at the open eastern and southern boundaries of the target domain. Linear combinations of these Green's functions synthesize dynamic boundary conditions at the target-domain boundaries, allowing us to avoid ~8 h of the large-domain propagation while preserving dispersion.

In the second step, we generate an ensemble by perturbing the source with Gaussian slip noise, obtain boundary conditions for each member via linear combinations of the boundary Green's functions, and run target-domain simulations. Using JAGURS nested grids, we apply the non-dispersive nonlinear shallow-water equations in shallow coastal nests including parts of the TIARES array and Papeete (PPT) and linear long-wave (non-dispersive) calculations elsewhere. The resulting flows drive TMTGEM (Minami et al., 2017) to simulate TGM fields. Within 4DEnVar, we estimate optimal Green's-function weights from the TGM data and iterate until residuals decrease sufficiently.

Combining these two steps preserves dispersion characteristics at the boundaries while enabling local nonlinear DA within the target domain. By integrating seafloor TGM data with nonlinear regional simulations, we aim to improve tsunami prediction accuracy in French Polynesia, and evaluate performance by comparing our prediction with pressure-gauge records at PPT.

津波が伝播する際に電気伝導性を有する海水が地球の地磁気場を通過すると、流体の流れと地磁気場との相互作用によって二次的な誘導磁場が生成される。このような津波によって生じる磁気場(TGM: Tsunami-Generated Magnetic field)は、海底で観測されている(Toh et al., 2011; Suetsugu et al., 2012)。また、理論研究と観測データの蓄積により、TGM に関する理解は近年大きく進展している(例: Tyler, 2005; Minami et al., 2015; 2021)。圧力データとは異なり、TGM 場は単一点における三成分計測から津波の伝播方向を推定可能である(Sugioka et al., 2014; Lin, 2024)。この特性は、津波予測と災害軽減策の向上に寄与する可能性を秘めている。

データ同化(DA)は観測データと数値シミュレーションを統合してリアルタイム予測を行う強力な手法であり、気象

予報分野で広く活用されている。近年の研究では、線形長波モデルと圧力データを用いた津波予測への応用が実証されている(Maeda et al., 2015)。しかしながら、これまでの津波 DA 研究では主に線形モデルと圧力データが用いられており、海底 TGM データを同化する手法や、浅海域で顕著となる非線形効果を明示的に考慮した研究は報告されていない。

本研究では、津波の非線形性を考慮した DA 手法を実装し、フランス領ポリネシアにおける 2010 年チリ地震津波時の地域津波場予測において、海底磁気観測データを同化することで TGM 場の有用性を評価する。当該事象発生時には、TIARES が設置した 9 台の海底電磁気計(OBEM)と 1 台の差圧計(DPG)によって磁気信号と圧力信号が記録されている(Suetsugu et al., 2012; Sugioka et al., 2014)。複雑な多島海の海底地形に起因する強い非線形効果により、シミュレーション結果と DPG 記録との間には、到達時間と振幅において不一致が生じていることが報告されている(Lin et al., 2021)。 TGM 場は単一点における三成分計測によって伝播方向情報を提供するため、圧力データ単独と比較して予測効率と精度の向上が期待できる。

本研究では、前方モデルと疎な観測データを結合する 4 次元アンサンブル変分法(4DEnVar: Liu et al., 2008)を採用する。この手法は接線線形/随伴モデルを仮定せず、弱い非線形性を前提とすることで、アンサンブルベースの背景誤差推定と反復更新を可能にする。

効率性と物理性(分散性と非線形性)のバランスを取るため、我々は2領域・2段階の戦略を採用する。具体的には、対象領域をより大きな領域内に埋め込む。この領域には、発生源領域と対象領域の両方が含まれる。第1段階では、2010年の発生源モデル(Yoshimoto et al., 2016)の各副断層に単位滑り量を仮定した44回の分散考慮型JAGURSシミュレーション(Baba et al., 2017)を実施し、対象領域の東側開放境界と南側開放境界における海面変位時系列への単位滑り量のマッピングを行うグリーン関数を事前に計算する。これらのグリーン関数の線形結合により、対象領域境界における動的境界条件を合成することで、大規模領域での伝播時間約8時間を省略しつつ、分散特性を保持することが可能となる。

第2段階では、Yoshimoto et al. (2016) の発生源モデルにガウス分布に従う滑りノイズを付加してアンサンブルを生成し、各メンバーに対する境界条件を境界グリーン関数の線形結合によって取得する。その後、対象領域におけるシミュレーションを実行する。JAGURS の入れ子グリッド構造を活用し、TIARES アレイの一部と主要評価地点である TIARES アレイ近傍のパペーテ(PPT)を含む浅海域の沿岸入れ子領域では非分散型の非線形浅水方程式を、それ以外の領域では線形長波(非分散)計算を適用する。得られた流体運動を用いて TMTGEM(Minami et al., 2017)を駆動し、TGM 場をシミュレーションする。4DEnVar の枠組み内では、TGM データから最適なグリーン関数の重みを推定し、残差が十分に減少するまで反復計算を行う。

この2段階の手法により、境界領域における分散特性を保持しつつ、対象領域内で局所的な非線形DAを実施することが可能となる。海底TGMデータを非線形地域シミュレーションと統合することで、フランス領ポリネシアにおける津波予測精度の向上を図り、PPTにおける圧力計記録との比較を通じて予測性能を評価する。